

New Aspects of H₂ Activation by Nickel–Iron Hydrogenase

MARIA PAVLOV, MARGARETA R. A. BLOMBERG, PER E. M. SIEGBAHN

Department of Physics, Stockholm University, Box 6730, S-113 85 Stockholm, Sweden

Received 17 October 1998; revised 17 December 1998; accepted 19 December 1998

ABSTRACT: The density functional theory (DFT) method B3LYP has been used to investigate the catalytic mechanism of Ni–Fe hydrogenases in light of new experimental data on the structure. The reaction pathway suggested in previous theoretical work is now slightly modified. In the reaction mechanism proposed in the present study, one of the hydrogens from H₂ appears as a hydride bridge between Ni and Fe in the reduced form. The bridging hydride brings Ni and Fe closer together, which results in an interatomic distance of 2.56 Å, which is a shortening from the calculated oxidized form of 0.28 Å. A shortening of the Ni–Fe distance in the reduced form as compared to the oxidized form agrees with the recent experimental X-ray structures. Effects on the reaction mechanisms, due to protonation and deprotonation of the terminal cysteine ligands on Ni and coordination of a water molecule on Ni have also been studied. Solvent effects have been included using dielectric cavity methods. © 1999 John Wiley & Sons, Inc. *Int J Quant Chem* 73: 197–207, 1999

Key words: Ni–Fe hydrogenase; density functional theory

Introduction

Hydrogenases are enzymes that catalyze the reversible oxidation of molecular hydrogen ($\text{H}_2 \rightleftharpoons 2\text{H}^+ + 2e^-$). The products formed in the H₂ activation can be used by bacteria for reduction of inorganic molecules such as CO₂, SO₄²⁻, NO₃⁻, and O₂. For hydrogenases located on the bacterial membrane a transmembrane proton gradient can be created which leads to adenosine triphosphate

Correspondence to: M. Pavlov.

(ATP) formation. In that way, many microorganisms can use hydrogen gas as a source of energy.

The majority of hydrogenases contain iron atoms arranged in Fe–S clusters, and many of them also contain one nickel atom in the active site. The nickel-containing enzymes are termed Ni–Fe hydrogenases or, if a selenium atom is present as a ligand to Ni in the active site, Ni–Fe–Se hydrogenases. The other types of hydrogenases are Fe-only hydrogenases, containing Fe–S clusters but not nickel, and a recently observed hydrogenase, which neither contains nickel nor Fe–S clusters [1]. Most

Ni-Fe hydrogenases catalyze the forward reaction in which H_2 is consumed [2]. For Ni-Fe hydrogenases in some bacteria, i.e., *Desulfovibrio gigas* [3, 4] and *Thiocapsa roseopersicina* [5], the reaction can also be driven in the opposite direction. However, Ni-Fe hydrogenases usually catalyze H_2 consumption at a higher rate than H_2 production [2].

The first X-ray crystal structure obtained for a hydrogenase was solved at 2.85 Å resolution by Volbeda et al. [6] for the inactive air-oxidized form of the Ni-Fe hydrogenase from *D. gigas*. A nickel atom and also a second metal atom close to nickel were located in the active site. In Ref. [6] it was tentatively identified as an iron atom. Later, a new structure was obtained at a higher resolution of 2.54 Å [7], which led to the conclusion that the second metal atom in the active site has to be iron. The Ni-Fe cluster consists of a Ni bound to four Cys thiolates, two of which are bridging to the Fe atom. An additional oxygen-containing bridge between Fe and Ni is considered to be associated with the oxidized inactive form of the enzyme. This group is removed upon reduction to the active forms. The asymmetry of the bridge (Ni-O, 1.7Å; Fe-O, 2.1Å) has led to the suggestion that a Ni = O → Fe bridge is present [7]. Recent quantum chemical results are not in agreement with this assignment and instead an OH bridge is proposed [8]. In addition to the cysteine ligands and the oxygen-containing ligand, the iron atom is coordinated to three nonprotein diatomic molecules. Spectroscopic infrared (IR) studies [9] identified these ligands as two CN and one CO. A schematic diagram of the active site of the oxidized form of Ni-Fe hydrogenase is shown in Figure 1(a). The ligand positioned trans to the oxygen bridge has been suggested to be CO due to its hydrophobic environment [7].

Several different enzyme states have been observed for the Ni-Fe hydrogenases. Under aerobic conditions, an inactive form is isolated which can show two types of electron paramagnetic resonance (EPR) signals, an unready form known as Ni_u^* (also referred to as Ni-A) and a ready form, Ni_r^* (Ni-B), as well as two EPR-silent forms, Ni_u^-S and Ni_r^-S (Ni-S). The ready forms can be rapidly activated by H_2 in the presence of certain electron carriers, to give the active form that shows the Ni_a-C^* EPR signal. Reduction or oxidation of this form yields two further EPR-silent forms, Ni_a-S (Ni-S_{II}) and Ni_a-R-S (Ni-R). Illumination of the Ni_a-C^* form gives another EPR-visible form

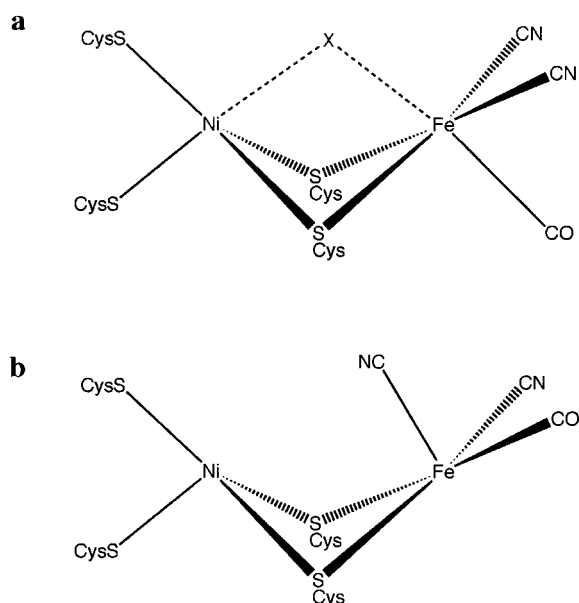


FIGURE 1. Schematic diagrams of the active site of Ni-Fe hydrogenase. (a) Structure based on X-ray data [7] and IR data [9]. In the oxidized form of the enzyme, an oxygen-containing ligand (X) forms a bridge between nickel and iron. In the reduced active form, this ligand is here proposed to be replaced by a hydride. (b) Structure obtained from geometry optimization in the gas phase for a form of hydrogenase where the oxygen-containing ligand has been removed. This structure was used as a working model in the previous quantum chemical study of Ni-Fe hydrogenase [13].

termed Ni_a-L^* . The Ni_u^* form is only activated by H_2 over several hours.

Based on experimental work, several mechanisms have been proposed for the Ni-Fe hydrogenase over the years [7, 10–12]. Recently, the first quantum chemical study on this system was carried out [13]. The knowledge of the structure for the oxidized enzyme, Ni_u^* , given from the X-ray crystallographic studies [7] together with the spectroscopic assignment of the diatomic ligands [9] had made theoretical calculations on the active site feasible. However, no structures were available for the forms of the enzyme directly involved in the H_2 dissociation when the first theoretical investigations were carried out. In Ref. [13], the positions of the active site ligands for these forms were determined from quantum chemical calculations on a model cluster containing nickel, iron, the four cysteines (modeled as SH^- or SH_2), and the diatomic CN^- and CO ligands. In these calculations, the orientation of the CO and CN ligands, as

shown in Figure 1(b), gives the lowest energy [13]. This means that one of the CN ligands points toward Ni, resulting in a weak interaction between these two. However, the energy difference between different orientations of the diatomic ligands for the intermediates involved in the H-H activation is rather small, on the order of 5 kcal/mol, which indicates that rotations of these groups could easily be hindered by hydrogen bonds to adjacent amino acid residues not represented in the theoretical model. In Ref. [13], all plausible reaction pathways and oxidation states were investigated. Since the reaction is known to be reversible, it should be close to thermoneutral. Furthermore, the activation energy is determined experimentally to be about 10 kcal/mol [14]. It turned out that H₂ could only be activated with a barrier of this size by a state of the Ni-Fe cluster that has an odd number of electrons. Since it could not be determined from the calculations if this state is best described as Fe(II)Ni(III) or as Fe(III)Ni(II), it is here denoted Ni,Fe(III,II). Furthermore only one reaction pathway was found for the H₂ activation. Several attempts were made to find molecular H₂ precursors at both metal centers, but the only site where H₂ was found to bind significantly was on iron. A transition state for the H-H dissociation giving an activation energy of 8.7 kcal/mol was found, leading to an intermediate with one hydride binding to iron and the other hydrogen binding as a proton to a bridging cysteine thiolate group. As this happens, the protonated cysteine ligand dissociates from nickel, giving an overall exothermicity of the dissociation of 3.5 kcal/mol relative to the H₂ precursor. This reaction mechanism is in agreement with isotope exchange experiments, indicating that H₂ is cleaved heterolytically by hydrogenase, into a hydride (H⁻), that could bind to a metal, and a proton (H⁺), that could be accepted by an adjacent base after the reaction.

In addition to the first experimental structure available for the oxidized form, a new structure has recently been obtained for a reduced form of the Ni-Fe-Se hydrogenase from *D. baculatum* [15]. An interesting feature of the new structure is that the distance between iron and nickel is significantly shortened compared to the oxidized form. Another feature of the new structure is that the diatomic ligands were shown to be positioned in an orientation quite similar to that of the oxidized form of the *D. gigas* enzyme; see Figure 1(a). This new experimental information has led us to a

reinvestigation of the H₂ activation mechanism in Ni-Fe hydrogenase. As will be described below, slight modifications of the mechanism suggested in Ref. [13] are obtained.

Computational Details

The calculations were performed in two steps. First, an optimization of the geometry was performed using the B3LYP method [16, 17]. Double-zeta basis sets were used in this step. In the second step the energy was evaluated for the optimized geometry using large basis sets including diffuse functions and with a single set of polarization functions on each atom. The final energy evaluation was also performed at the B3LYP level. All the calculations were carried out using the GAUSSIAN programs [18, 19].

In the B3LYP geometry optimizations, the LANL2DZ set of the GAUSSIAN-94 program, was used. For the iron, nickel, and sulfur atoms this means that a nonrelativistic effective core potential (ECP) according to Hay and Wadt [20] was used. The metal valence basis set used in connection with this ECP is essentially of double-zeta quality. The rest of the atoms are described by standard double-zeta basis sets. The Mulliken population analysis computed at this level gives the spin distributions. In the B3LYP energy calculations the diffuse and polarization functions from the 6-311 + G(1d,1p) basis sets in the GAUSSIAN-94 program were added to the LANL2DZ basis sets. This basis set has a single set of polarization functions on all atoms including *f*-sets on the metals, and also diffuse functions. For the neutral model clusters that will be discussed below and shown in Figure 2, zero-point vibrational effects were calculated at the same level as the geometry optimization using the GAUSSIAN-98 program. The zero-point effects have been assumed to be the same for other models. These effects have been added to the final energies.

The dielectric effects from the surrounding protein were obtained using the self-consistent reaction field (SCRf) method [21]. This is one of the simplest models for treating long-range solvent effects and considers the solvent as a macroscopic continuum with a dielectric constant ϵ and the solute as filling a cavity in this continuous medium. In the present study the self-consistent isodensity polarized continuum model (SCI-PCM) as implemented in the GAUSSIAN-94 program has been

CO and CN ligands, as indicated in Figure 1(b). Then the catalytic cycle of Ni-Fe hydrogenase will be discussed. A correlation between calculated and experimentally observed structures is proposed. A discussion of the effects of using charged model clusters will follow. In the final section results obtained for the addition of a coordinating water molecule to a terminal position on nickel will be described.

MECHANISM OF H₂ ACTIVATION

As discussed in Ref. [13], a neutral model cluster is in general preferred for the present type of modeling. Charged models are, for example, frequently found to be unstable toward dissociation into fragments due to strong electrostatic repulsion. The desired oxidation states can be achieved within a neutral model by using a proper number of anionic and neutral ligands. In the present case of cysteine ligands, for simplicity SH⁻ is used as the anionic model and H₂S as the neutral model. Since one of the bridging cysteine ligands was found to be directly involved in the reaction, a small correction based on calculations for an improved model using an SCH₃⁻ for that ligand has been added to the final results. As mentioned in the introduction, only one oxidation state, Ni,Fe(III,II), was found to activate H₂ in the previous quantum chemical study of the Ni-Fe hydrogenase [13]. Using a neutral model cluster, this means modeling one of the cysteine ligands as SH₂ and the remaining three as SH⁻ (see Fig. 2). If nothing else is stated, this model has been used for the results reported below.

The spin state for the Ni-Fe center in the EPR-visible states is $S = \frac{1}{2}$. In the present study, calculations for some of the structures have been performed both for $S = \frac{1}{2}$ and $S = \frac{3}{2}$ clusters, resulting in very similar structures and energies. In most cases, the main difference is the opposite orientation of the spins on iron and nickel in the $S = \frac{1}{2}$ solutions. Since convergence problems were present for some of the calculations on the low-spin clusters, the results will be reported only for clusters with $S = \frac{3}{2}$. The procedure of using high-spin states in density functional theory (DFT) (B3LYP) calculations for bimetallic systems has successfully been used before [24, 25]. Since magnetic data indicate that the iron is low-spin ferrous for most enzyme states [12, 26], further investigations of $S = \frac{1}{2}$ states are in progress.

In the inactive form of the enzyme, the position trans to the CO ligand on Fe is occupied by an oxygen-containing bridging ligand [Fig. 1(a)], which is removed upon activation. The recent X-ray crystal structure indicates that the CO and CN ligands do not rotate upon activation. Then the only site on Fe where H₂ can bind and react is at the position previously occupied by the oxygen-derived ligand. Similar to what was obtained for the cluster with the CO and CN ligands as in Figure 1(b) [13], a bound molecular H₂ precursor could only be located at the Fe site. The optimized structure is shown in Figure 2(a). Attempts to find H₂ complexes on both the Ni and at a bridging site between the metals were made but no binding was obtained at these positions.

The structure, depicted in Figure 2(a), shows a quite long Ni-Fe distance of 3.40 Å, compared to 2.9 Å in the crystal structure [7], and also compared to our calculated results for the oxidized form [8], where the Ni-Fe distance is 2.84 Å. The presence of an OH bridge in the oxidized form shortens the Ni-Fe distance, and since no such bridge is present in the structure shown in Figure 2(a), the distance between the metals becomes longer. In previous theoretical models [13] one of the CN ligands occupied the bridging site, and therefore an elongation of the Ni-Fe distance was not obtained.

In the reaction pathway proposed in Ref. [13], a hydride binds to iron and a proton is transferred to one of the bridging cysteine ligands in the product after the H₂ activation. However, as discussed above, this does not lead to a structure with a sufficiently short Ni-Fe distance to be in accordance with the recent X-ray structure [15]. Rather than a hydride binding to Fe only, the short Ni-Fe distance could be explained by a formation of a hydride bridge between the metals, which has in fact been suggested before [7, 12]. This would also be consistent with the orientation of the CO and CN ligands observed for the reduced form. The results using the model in Figure 2(a) is that the structure for the product formed after the transition state is passed indeed has a bridging hydride, as shown in Figure 2(c). For the model used in the present calculations, protonation of the bridging cysteine causes a loss of coordination of this ligand to the nickel. The calculations indicate, however, that this movement yields a very small energy gain, which means that it might be hindered in the protein. The distance between nickel and iron in this state is 2.62 Å, thus substantially shortened in

agreement with experiments. The calculated shortening is 0.22 Å with respect to the calculated distance of 2.84 Å for the inactive oxidized form with a bridging OH group. It can furthermore be noted that the calculated Ni–Fe distance for the oxidized form is also in good agreement with the experimental value of 2.9 Å [7]. The position of the hydride bridge is slightly asymmetric, giving a distance to Fe of 1.60 Å and to Ni of 1.78 Å. However, it should be pointed out that we do not suggest that the immediate product of the dissociation is the one observed in the X-ray structure; see further below. The exothermicity obtained in the gas phase for the reaction involving the structures shown in Figure 2(a)–2(c) is 7.1 kcal/mol. Inclusion of dielectric effects from the surrounding protein decreases the exothermicity for the H₂ activation to a final value of 3.3 kcal/mol, which is close to thermoneutral, as it should be for a reversible reaction.

A transition state for an H–H cleavage, leading to a hydride bridge between nickel and iron and a protonated bridging cysteine, was located resulting in the structure shown in Figure 2(b). Already at the transition state the distance between the metals is rather short, 2.78 Å, due to the bridge that is being formed between the metals, giving a distance from the hydride to the nickel and the iron of 2.07 Å and 1.69 Å, respectively. At the same time, the H–H bond in H₂ is elongated and cysteine starts to interact with one of the hydrogens from H₂. The activation energy for this step is in the gas phase for the model shown in Figure 2(b), 11.7 kcal/mol. In Ref. [13], the use of SCH₃⁻, instead of SH⁻, for the bridging cysteine ligand directly involved in the H₂ activation was shown to lower the activation energy by 2.3 kcal/mol. Methyl substitution is estimated to have the same effect on the energetics for the reaction path proposed in the present study since it is only slightly different from the path suggested in Ref. [13], leading to an activation energy of 9.4 kcal/mol. Inclusion of polarization effects from the surrounding protein on the other hand raises the barrier, leading to a final value for the H₂ activation energy of 14.7 kcal/mol, which is somewhat higher than the corresponding experimental value of 10 kcal/mol [14]. The solvent effect obtained using the SCI-PCM method should, however, be regarded as somewhat uncertain since the hydrogen bonds from the CN ligands to the arginine and serine are not present explicitly in the model. Previous studies indicate that ideally the hydrogen

bonds that are binding directly to the cluster should be included quantum mechanically [23].

A transition state was also located for a dissociation on nickel where one proton from H₂ is accepted by one of the cysteines terminally bound to the Ni and the remaining hydride becomes bridging between the metals. The activation energy obtained for that dissociation is 8.8 kcal/mol higher than the dissociation discussed above, corresponding to a reaction rate that is slower by a factor of 10⁶. A dissociation on nickel is therefore considered very unlikely.

CATALYTIC CYCLE

From the results presented above, it is possible to make a preliminary proposal for a catalytic cycle of Ni–Fe hydrogenase as shown in Figure 3. The key computational result on which this proposal is built is that only one complex has been found to activate H₂. This active complex has an odd number of electrons and should thus be EPR-active. No EPR-inactive state has so far been found to activate H₂. Apart from the H₂ activation, the catalytic cycle should just involve restoring the complex to the original form by sending the electrons obtained from H₂ to the iron–sulfur acceptors and sending the H₂ protons away along the proton transfer channels. For simplicity the disposal of electrons and protons are assumed to be strongly coupled in two separate steps, so that the complex keeps the same charge. In the first three steps of the cycle one hydrogen molecule is activated. This leads from the upper right corner in Figure 3 to the lower left corner. As mentioned in the introduction, several different forms of the enzyme have been observed experimentally based mainly on EPR and Fourier transform infrared (FTIR) experiments. During catalytic turnover, two EPR-visible species, Ni_a-C* and Ni_a-L*, and two EPR-silent species, Ni_a-R-S and Ni_a-S, are observed. Our suggestion for the EPR-silent Ni_a-R-S intermediate is shown in Figure 2(d) and also marked in Figure 3. It is this “fully reduced” form that gives the major contribution to the new crystal structure of the active enzyme [15]. Our assignment is mainly built on the fact that a short Ni–Fe distance is observed in the crystal structure, which according to our calculations requires the presence of a bridging hydride. The calculated distance between iron and nickel for this form is only 2.56 Å and thus shortened by 0.28 Å from the form containing the hydroxo bridge. The hydrogen

bridge is still present and two SH⁻ groups form bridges between the metals. Both the reactant (upper right corner in Figure 3) and the product structure (lower left corner) have an odd number of electrons and are thus candidates for the EPR-visible intermediates observed. Since the H₂ activation should be exothermic and experiments indicate that Ni_a-C* is the most stable EPR-visible species observed, we assign the product structure to be Ni_a-C*. This leaves the possibility that Ni_a-L* should be assigned as the reactant or as an isomer of the product, for example, with the hydride moved over to the nickel side. In order to assign the second EPR-silent intermediate observed, Ni_a-S, an isoelectronic isomer to Ni_a-R-S is finally needed. It is suggested that this isomer has a hydrogen on a terminal Ni-cysteine instead of a bridging hydride.

CHARGED MODELS

To use a neutral model cluster is a natural choice since charges are not in general stabilized in

the low dielectric medium of the core of the enzyme where the catalytic center is hidden. This constraint on the model may anyway be questioned since *small* variations of the charge in the protein are likely to be present. Therefore, in addition to neutral clusters also models with overall charges of +1 and -1 have been tested for the structures involved in the H₂ dissociation. For the positively charged model this means adding a proton (H⁺) to the unprotonated Cys ligand terminally bound to the Ni in the structures shown in Figure 2. The negatively charged model is obtained in a similar way by removing a proton from the protonated terminal Cys ligand. The number of electrons is thus the same for all these models. Structural parameters, spin populations, and relative energies for clusters with different charges are given in Tables I, II, and III.

For the molecular hydrogen complex, all properties are quite similar for the three differently charged models. They all have a long distance between nickel and iron of about 3.4 Å, and the

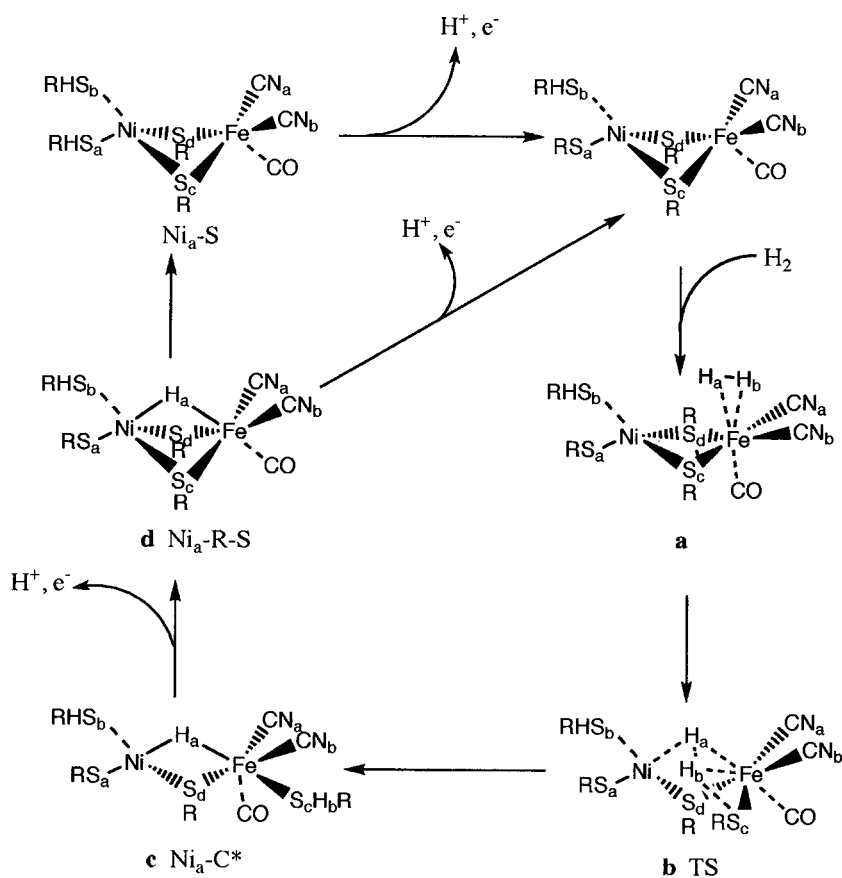


FIGURE 3. Proposed catalytic pathway for Ni-Fe hydrogenase.

TABLE I

Interatomic distances [$d(A,B)$] between atom A and B in Å using different models for structures along the reaction pathway for H₂ dissociation.^a

	[NiS ₄ H ₆ FeC ₃ N ₂ O] ⁻			NiS ₄ H ₇ FeC ₃ N ₂ O			[NiS ₄ H ₈ FeC ₃ N ₂ O] ⁺		
	<i>a</i>	<i>b</i>	<i>c</i>	<i>a</i>	<i>b</i>	<i>c</i>	<i>a</i>	<i>b</i>	<i>c</i>
$d(Ni,S_a)$	2.31	2.44	2.46	2.25	2.26	2.26	2.50	2.47	2.49
$d(Ni,S_b)$	2.35	2.46	2.47	2.58	2.55	2.56	2.52	2.47	2.48
$d(Ni,S_c)$	2.52	—	—	2.48	—	—	2.42	—	—
$d(Ni,S_d)$	2.49	2.44	2.48	2.44	2.52	2.56	2.38	2.39	2.41
$d(Ni,H_a)$	—	1.92	1.70	—	2.07	1.77	—	2.14	1.70
$d(Ni,Fe)$	3.35	2.70	2.59	3.40	2.78	2.62	3.46	2.82	2.78
$d(Fe,S_c)$	2.39	2.54	2.45	2.42	2.47	2.46	2.46	2.41	2.50
$d(Fe,S_d)$	2.42	2.49	2.46	2.43	2.40	2.38	2.46	2.46	2.44
$d(Fe,H_a)$	1.91	1.73	1.68	1.86	1.69	1.59	1.86	1.67	1.63
$d(Fe,H_b)$	1.78	1.84	—	1.86	1.83	—	1.86	1.86	—
$d(H_a,H_b)$	0.78	1.07	—	0.78	1.01	—	0.77	1.10	—
$d(H_b,S_c)$	—	1.67	1.37	—	1.74	1.37	—	1.68	1.37

^a The notation refers to Figure 3.

TABLE II

Mulliken atomic spin populations using different models for structures along the reaction pathway for H₂ dissociation.^a

	[NiS ₄ H ₆ FeC ₃ N ₂ O] ⁻			NiS ₄ H ₇ FeC ₃ N ₂ O			[NiS ₄ H ₈ FeC ₃ N ₂ O] ⁺		
	<i>a</i>	<i>b</i>	<i>c</i>	<i>a</i>	<i>b</i>	<i>c</i>	<i>a</i>	<i>b</i>	<i>c</i>
S(Ni)	1.47	1.40	1.39	1.37	1.32	1.31	1.47	1.45	1.43
S(Fe)	1.05	0.04	0.14	1.06	1.13	1.21	1.00	1.12	1.20
S(S _a)	0.22	0.65	0.59	0.43	0.44	0.39	0.09	0.11	0.12
S(S _b)	0.14	0.66	0.69	0.03	0.07	0.07	0.02	0.07	0.05
S(S _c)	0.11	0.05	0.00	0.10	0.00	0.02	0.28	0.02	-0.03
S(S _d)	0.11	0.16	0.13	0.08	0.12	0.14	0.14	0.19	0.23

^a The notation refers to Figure 3.

TABLE III

Relative energies (ΔE) given in kcal / mol for H – H activation by Ni – Fe hydrogenase using different models.^a

Structure	ΔE (gas phase)	ΔE (including solvent)
SH ₂ NiSH-(SH) ₂ -Fe(H ₂)(CN) ₂ CO	0.0	0.0
Transition state	+9.4	+14.7
SH ₂ NiSH-(SH)(CN)-FeH(SH ₂)(CN)(CO)	-7.1	-3.3
[SHNiSH-(SH) ₂ -Fe(H ₂)(CN) ₂ CO] ⁻	0.0	0.0
Transition state	+19.8	+18.6
[SHNiSH-(SH)(CN)-FeH(SH ₂)(CN)(CO)] ⁻	+14.8	+11.7
[SH ₂ NiSH ₂ -(SH) ₂ -Fe(H ₂)(CN) ₂ CO] ⁺	0.0	0.0
Transition state	+7.1	+10.6
[SH ₂ NiSH ₂ -(SH)(CN)-FeH(SH ₂)(CN)(CO)] ⁺	-5.6	-3.5
(SH ₂)(OH ₂)NiSH-(SH) ₂ -Fe(H ₂)(CN) ₂ CO	0.0	0.0
Transition state	+3.1	+6.4
(SH ₂)(OH ₂)NiSH-(SH)(CN)-FeH(SH ₂)(CN)(CO)	-6.1	-3.1

^a The energies are taken relative to the model for the H₂ precursor that has the same number of protons.

deviations in the spin population distributions are also small. The main difference between the models of the H₂ complex concerns the distances between Ni and the individual cysteine ligands. However, the average Ni-S-Cys distance in the charged clusters deviates only by 0.02 Å from the neutral model. Transition states were located for all three charge states of the model. From Table III one can see that protonation lowers the barrier, from 14.7 kcal/mol to 10.6 kcal/mol including dielectric effects from the surrounding protein. Deprotonation instead raises the barrier, and for this model an activation energy of 18.6 kcal/mol was obtained. The reaction energy obtained for the positively charged cluster is 3.5 kcal/mol, compared to the value of 3.3 kcal/mol obtained for the neutral cluster. For the negatively charged model, the reaction is *endothermic* by 11.7 kcal/mol. The negatively charged model cluster used in the present study does thus not seem to be a good model for the H₂ activating complex from an energetics point of view; a too high barrier was obtained, the reaction is too *endothermic*, and furthermore unexpectedly large spin densities were observed on the cysteine sulfurs (see Table II). On the other hand, the positively charged complex seems to be a somewhat better model than the neutral one if the energetics are considered.

FURTHER MODEL ASPECTS

Results from calculations on different models of inactive forms of the enzyme [8] indicate that formation of water in a bridging position between nickel and iron could occur in one of these forms. This water molecule could later be transferred to a terminal position on nickel. A series of calculations were set up to investigate what effect such a water ligand would have on the energetics, thus investigating a reaction path for a neutral model cluster similar to the one shown in Figure 2, but with an additional water coordinating to nickel. Starting with the molecular hydrogen complex, coordination of water has only minor effects on the structure. The largest effect concerns the Ni-S distances to the three cysteine ligands, which all become elongated, on average by 0.1 Å. This also affects the spin population on Ni, which increases from 1.37 to 1.50 when water is added. The spin population on the unprotonated Cys terminally bound to Ni on the other hand decreases from 0.43 to 0.26. The spin population of 1.06 on iron remains unaffected upon addition of water. Also the long Ni-Fe

distance of 3.4 Å is independent of coordination of water to nickel. The binding energy of the water molecule to the Ni-Fe complex is 6.2 kcal/mol.

When the water ligand is present, the H-H activation is found to take place only on iron. For the transition state including the water, a long nickel-hydride distance of 2.63 Å and also a long distance between iron and nickel of 3.39 Å was obtained. This long Ni-Fe distance originates from a hydrogen bond that is formed between one of the CN ligands on Fe and the water molecule. In the real enzyme, a nearby amino acid residue is expected to be hydrogen bonded to CN, preventing the hydrogen bonds to the water ligand. Investigations of an improved model of the active site, including the amino acid residues that form hydrogen bonds to CN, are in progress. The H₂ activation energy for the model which has a water molecule coordinated to Ni is only 6.4 kcal/mol including dielectric effects. The additional water thus has a large lowering effect (8.3 kcal/mol) on the activation energy. Also in the product of the H₂ activation, the distance between the metals is longer for the water-containing structure, 2.80 Å compared to 2.62 Å for the model without water. The reaction energy is, in contrast to the activation energy, very similar for the two models. The model, for which the coordinating water is present, gives an exothermicity for the H₂ dissociation of 3.1 kcal/mol compared to 3.3 kcal/mol for the model without water. In our model for the Ni_q-R-S form, which is the form that gives the major contribution to the new X-ray structure, no hydrogen bonds are formed between the CN ligands and the water molecule, and therefore addition of water does not significantly affect this structure [Fig. 2(d)]. When the water molecule is present, the Ni-Fe distance is only 2.58 Å, in good agreement with the fact that a short distance between Ni and Fe is observed in the new X-ray structure.

Conclusions

Inspired by a recent X-ray structure for a reduced form of the Ni-Fe-Se hydrogenase from *D. baculatum* [15], quantum chemical calculations have been performed in order to verify if a similar mechanism for the H-H dissociation in Ni-Fe hydrogenase as suggested previously [13] holds also if the model is slightly modified in accordance with the new experimental results. The modifica-

tion concerns the orientation of the CN and CO ligands. The present results agree with those obtained in Ref. [13] in several aspects: (i) Only one form, for which there is an odd number of electrons located on the Ni-Fe cluster, yielding the oxidation state Ni-Fe(III,II), was found to activate H₂, with reasonable energetics. (ii) A molecular hydrogen precursor was found only at the Fe site. (iii) After the activation, one of the hydrogens from H₂ appears as a proton accepted by one of the bridging sulfurs and the other hydrogen as a metal-bound hydride. The modification of the chemical model leads, however, to one difference. Instead of binding to iron only, the hydride forms a bridge between nickel and iron. The optimal bond distances between the hydride and the metals force the nickel and the iron closer together. In the product of the H-H dissociation, the Ni-Fe distance is 2.62 Å and in the fully reduced form (Ni_a-R-S) it is even shorter, 2.56 Å. Compared to results for a model of the oxidized form which has a bridging OH, this yields a total shortening of the Ni-Fe distance by 0.28 Å. A shortening of the distance between Ni and Fe in the reduced form compared to the oxidized form is in agreement with the new crystallographic results [15]. The present study shows that the short distance is an effect of the bridging hydride. In the gas phase, the activation energy and the reaction energy is +9.4 and -7.1 kcal/mol, respectively, using a neutral model.

The dielectric effects of the surrounding protein raise the activation energy for the neutral model to 14.7 kcal/mol and gives an exothermicity of 3.3 kcal/mol. These results can be compared to the experimental value for the activation energy of 10 kcal/mol and the known fact that the reaction should be close to thermoneutral. The large effects obtained by introducing the solvent are, however, somewhat uncertain since the hydrogen bonds between the active site ligands and nearby residues are not represented in the chemical model. The effect of adding or removing a proton from the terminal cysteine ligands in the neutral model, corresponding to models with total charges of +1 and -1, respectively, has also been investigated. The negatively charged model turns out to yield a too high barrier and a too large endothermicity, while the positively charged model well reproduces what is known about the energetics of the reaction, yielding an activation energy of 10.6 kcal/mol and an exothermicity of 3.5 kcal/mol, including effects from the surrounding dielectric

medium. The H-H activation has also been studied in the presence of a water molecule coordinating to nickel at a terminal position. For the model of the active site used in the present study, this water seems to significantly facilitate the reaction.

References

1. Thauer, R. K.; Klein, A. R.; Hartmann, G. C. *Chem Rev* 1996, 96, 3031.
2. Cammack, R. In *Bioinorganic Catalysis*, Reedijk, J., Ed.; Marcel Dekker: New York, 1993; pp. 189-225.
3. Cammack, R.; Patil, D. S.; Hatchikian, E. C.; Fernandez, V. M. *Biochim Biophys Acta* 1987, 912, 98.
4. Teixeira, M.; Moura, I.; Xavier, A. V.; Huynh, B. H.; Der Vartanian, D. V.; Peck, H. D.; LeGall, J. *J Biol Chem* 1985, 260, 8942.
5. Kovacs, K. L.; Bagyinka, C. *FEMS Microbiol Rev* 1990, 87, 407.
6. Volbeda, A.; Charon, M. H.; Piras, C.; Hatchikian, E. C.; Frey, M.; Fontecilla-Camps, J. C. *Nature* 1995, 373, 580.
7. Volbeda, A.; Garcin, E.; Piras, C.; de Lacey, A. L.; Fernandez, V. M.; Hatchikian, E. C.; Frey, M.; Fontecilla-Camps, J. C. *J Am Chem Soc* 1996, 118, 12989.
8. Pavlov, M.; Siegbahn, P. E. M.; Blomberg, M. R. A., to be published.
9. Happe, R. P.; Roseboom, W.; Pierik, A. J.; Albracht, S. P. J.; Bagley, K. A. *Nature* 1997, 385, 126.
10. Cammack, R.; Fernandez, V. M.; Schneider, K. In *The Bioinorganic Chemistry of Nickel*, Lancaster, J. R., Ed.; VCH: Weinheim, 1988; pp. 167-190.
11. Moura, J. J. G.; Teixeira, M.; Moura, I.; LeGall, J. *The Bioinorganic Chemistry of Nickel*, Lancaster, J. R., Ed.; VCH: Weinheim, 1988; pp. 191-224.
12. Dole, F.; Fournel, A.; Magro, V.; Hatchikian, E. C.; Bertrand, P.; Guigliarelli, B. *Biochemistry* 1997, 36, 7847.
13. Pavlov, M.; Siegbahn, P. E. M.; Blomberg, M. R. A.; Crabtree, R. H. *J Am Chem Soc* 1998, 120, 548.
14. McTavish, H.; Sayavedra-Soto, L. A.; Arp, D. *J Biochem Biophys Acta* 1996, 1294, 183.
15. Garcin, E.; Hatchikian, C.; Frey, M.; Fontecilla-Camps, J. C., in preparation.
16. Becke, A. D. *Phys Rev A* 1988, 38, 3098; Becke, A. D. *J Chem Phys* 1993, 98, 1372; Becke, A. D. *J Chem Phys* 1993, 98, 5648.
17. Stevens, P. J.; Devlin, F. J.; Chablowski, C. F.; Frisch, M. J. *J Phys Chem* 1994, 98, 11623.
18. Frisch, M. J.; Trucks, G. W.; Schlegel, H. B.; Gill, P. M. W.; Johnson, B. G.; Robb, M. A.; Cheeseman, J. R.; Keith, T.; Petersson, G. A.; Montgomery, J. A.; Raghavachari, K.; Al-Laham, M. A.; Zakrzewski, V. G.; Ortiz, J. V.; Foresman, J. B.; Cioslowski, J.; Stefanov, B. B.; Nanayakkara, A.; Challacombe, M.; Peng, C. Y.; Ayala, P. Y.; Chen, W.; Wong, M. W.; Andres, J. L.; Replogle, E. S.; Gomperts, R.; Martin, R. L.; Fox, D. J.; Binkley, J. S.; Defrees, D. J.; Baker, J.; Stewart, J. P.; Head-Gordon, M.; Gonzalez, C.; Pople, J. A. *Gaussian 94*, Revision B.2, Gaussian, Inc., Pittsburgh, 1995.

19. Frisch, M. J.; Trucks, G. W.; Schlegel, H. B.; Scuseria, G. E.; Robb, M. A.; Cheeseman, J. R.; Zakrzewski, V. G.; Montgomery, Jr., J. A.; Stratmann, R. E.; Burant, J. C.; Dapprich, S.; Millam, J. M.; Daniels, A. D.; Kudin, K. N.; Strain, M. C.; Farkas, O.; Tomasi, J.; Barone, V.; Cossi, M.; Cammi, R.; Mennucci, B.; Pomelli, C.; Adamo, C.; Clifford, S.; Ochterski, J.; Petersson, G. A.; Ayala, P. Y.; Cui, Q.; Morokuma, K.; Malick, D. K.; Rabuck, A. D.; Raghavachari, K.; Foresman, J. B.; Cioslowski, J.; Ortiz, J. V.; Stefanov, B. B.; Liu, G.; Liashenko, A.; Piskorz, P.; Komaromi, I.; Gomperts, R.; Martin, R. L.; Fox, D. J.; Keith, T.; Al-Laham, M. A.; Peng, C. Y.; Nanayakkara, A.; Gonzalez, C.; Challacombe, M.; Gill, P. M. W.; Johnson, B.; Chen, W.; Wong, M. W.; Andres, J. L.; Gonzalez, C.; Head-Gordon, M.; Replogle, E. S.; Pople, J. A. *Gaussian 98, Revision A.1*, Gaussian, Inc., Pittsburgh, 1998.
20. Hay, P. J.; Wadt, W. R. *J Chem Phys* 1985, 82, 299.
21. Wiberg, K. B.; Keith, T. A.; Frisch, M. J.; Murcko, M. *J Phys Chem* 1995, 99, 9072.
22. Blomberg, M. R. A.; Siegbahn, P. E. M.; Babcock, G. T. *J Am Chem Soc* 1998, 120, 8812.
23. Siegbahn, P. E. M.; Blomberg, M. R. A.; Pavlov, M. *Chem Phys Lett* 1998, 292, 421.
24. Siegbahn, P. E. M.; Crabtree, R. H. *J Am Chem Soc* 1997, 119, 3103.
25. Siegbahn, P. E. M.; Westerberg, J.; Svensson, M.; Crabtree, R. H. *J Phys Chem* 1998, B102, 1615-1623.
26. Huyett, J. E.; Carepo, M.; Pamplona, A.; Franco, R.; Moura, I.; Moura, J. J. G.; Hoffman, B. M. *J Am Chem Soc* 1997, 9291.